Optimal squeezing of vibrational wave packets in sodium dimers

D. G. Abrashkevich, I. Sh. Averbukh, and M. Shapiro

Citation: The Journal of Chemical Physics **101**, 9295 (1994); doi: 10.1063/1.467960
View online: http://dx.doi.org/10.1063/1.467960
View Table of Contents: http://scitation.aip.org/content/aip/journal/jcp/101/11?ver=pdfcov
Published by the AIP Publishing

Optimal squeezing of vibrational wave packets in sodium dimers

D. G. Abrashkevich, I. Sh. Averbukh, and M. Shapiro
Department of Chemical Physics, The Weizmann Institute of Science, Rehovot, 76100 Israel

(Received 17 May 1994; accepted 23 August 1994)

We present an application of "optimal squeezing" theory to the design of laser pulses for generation of squeezed states of material waves (states whose localization in some variable exceeds that of the ground state) in Na_2. Spatiotemporal evolution of the squeezed states during and after the laser pulse is studied. We show that the optimized laser pulses can affect squeezing via three basic scenarios whose realizations depend on the desired position of the wave packet and target squeezing times. These scenarios are alternations between momentum-space and coordinate-space squeezing, interfering collisions between wave packets, and overtaking of a slow front by a fast tail. © *1994 American Institute of Physics.*

I. INTRODUCTION

Considerable attention is being devoted in recent years to the generation of "squeezed" light, i.e., light for which the noise in one of the system variables is less than that of the vacuum state.[1] For some time, it has been realized[2–5] that squeezed material waves, for which the spread in some dynamical variable is less than that of the system ground state, can also be generated.

Recently, we have shown,[6] using optimal control techniques,[7–14] how such squeezing can be maximized with the aid of classical light pulses. The method developed called "optimal squeezing" involves a two-step numerical procedure that reduces the nonlinear optimization task to the solution of an eigenvalue problem. So far we have only applied the method to the generation of squeezed wave packets on model (shifted harmonic) potentials.

The interest in squeezing of molecular wave packets stems from recent experiments such as "pump–probe" femtosecond transition-state spectroscopy.[15,16] In these experiments, an excitation ("pump") pulse creates a wave packet on an excited, often dissociative, electronic state. This wave packet is probed either by a second (probe) pulse,[15] which dissociates or further excites the wave packet after an appropriate time delay, or by its spontaneous emission.[16] In this way, excited state dynamics can be followed in "real time," leading in principle to the mapping of the underlying potentials.[17]

The ability to map potential surfaces using such techniques depends critically on the generation of highly localized wave packets. Lacking such localization, the one-to-one correspondence between the delay time and the center of the wave packet in coordinate space is lost.[18] One can show,[19] using completeness arguments, that if minimum uncertainty pulses are used, an energetic bandwidth greater than that of the whole electronic absorption band is needed in order to generate a wave packet which mimics in shape the initial state. Since for many dissociative molecular systems the electronic absorption bands extend over thousands of wave numbers,[20] unrealistically short pulses would be needed. In contrast, if the pulse is shaped,[21,22] i.e., it is not a minimum uncertainty pulse, one can in fact squeeze the wave packet.[6]

In this paper, we present the first application of "optimal squeezing" theory[6] to *realistic* molecules. We have studied Na_2, for which observations of nonclassical vibrational wave packets have been recently made.[16] The paper is organized as follows: In Sec. II we describe briefly the optimal squeezing methodology. In Sec. III, we apply the method to squeezing in sodium dimers and discuss several squeezing scenarios. We summarize our results in Sec. IV.

II. OPTIMAL SQUEEZING METHODOLOGY

In this section, we briefly describe the essence of optimal squeezing methodology as developed in Ref. 6. We consider a situation in which a laser pulse excites a molecule, initially (at time $t=0$) in the ground vibrational state $|g\rangle$, to a manifold spanned by $|n\rangle$—a set of excited bound vibrational eigenstates (with energies E_n) of the radiation-free Hamiltonian. During the laser pulse, we expand the wave function of the system as

$$|\Psi(t)\rangle = C_g(t)|g\rangle\exp(-iE_g t) + \sum_n C_n(t)|n\rangle\exp(-iE_n t), \tag{1}$$

where atomic units ($\hbar=1$) are used throughout. The time dependence of the laser field can be written as

$$\epsilon(t) = f(t)\exp(-i\Omega t) + \text{c.c.}, \tag{2}$$

where Ω is the carrier frequency of the pulse, $f(t)$ is the pulse envelope (to be determined by the optimization procedure), and c.c. stands for complex conjugate.

Assuming that the laser field is weak, we may use first-order perturbation theory to calculate the $C_n(t)$ coefficients. In the Franck–Condon approximation we have that

$$C_n(t) = -i\mu\langle n|g\rangle\int_0^t dt' f(t')\exp(-i\Delta_n t'), \tag{3}$$

where

$$\Delta_n = \Omega + E_g - E_n .$$

In the spirit of the Franck–Condon approximation, μ is an average electronic transition dipole moment.

Our goal is to design laser pulses which maximize the degree of squeezing of the molecular wave packets at the end of an optimization time interval $(0,T)$ with T chosen at will.

The spatial spread of the excited state wave packet is measured by the mean-square deviation $\mathscr{D}$ of the wave packet from its average coordinate $\bar{x}$. The spread at the target time T is given as

$$\mathscr{D}=\frac{\langle\Psi'(T)|\hat{x}^2|\Psi'(T)\rangle-\langle\Psi'(T)|\hat{x}|\Psi'(T)\rangle^2}{\langle\Psi'(T)|\Psi'(T)\rangle}, \tag{4}$$

where $\Psi'(t)$ denotes the excited portion of the wave packet, i.e.,

$$\Psi'(t)=\sum_n C_n(t)|n\rangle\exp(-iE_nt). \tag{5}$$

Since the shape of the final wave packet does not depend on its normalization, we choose, for the sake of simplicity, to normalize $\Psi'(T)$ at the target time T to 1. Using the orthonormality of the $|n\rangle$ states, we have that

$$\langle\Psi'(T)|\Psi'(T)\rangle=\sum_n |C_n(T)|^2=1. \tag{6}$$

Introducing the notation

$$S_n(T)\equiv C_n(T)\exp(-iE_nT) \tag{7}$$

and using Eqs. (2) and (6), we can write for the average value of the position operator $\hat{x}$,

$$\bar{x}(T)\equiv\langle\Psi'(T)|\hat{x}|\Psi'(T)\rangle=\sum_{n',n} S^*_{n'}(T)(\hat{x})_{n',n}S_n(T), \tag{8}$$

and for average value of its square

$$\overline{x^2}(T)\equiv\langle\Psi'(T)|\hat{x}^2|\Psi'(T)\rangle=\sum_{n',n} S^*_{n'}(T)(\hat{x}^2)_{n',n}S_n(T), \tag{9}$$

where

$$(\hat{x})_{n',n}\equiv\langle n'|\hat{x}|n\rangle,$$
$$(\hat{x}^2)_{n',n}\equiv\langle n'|\hat{x}^2|n\rangle. \tag{10}$$

Since our *objective* is to generate a squeezed wave packet, we have to minimize the mean-square deviation $\mathscr{D}$. However, we also want to minimize the *cost*, which in our case is a "complicated-looking" pulse. We want to minimize this cost in order to simplify the pulse shaping task in practical applications. Mathematically speaking, a complicated looking pulse is characterized by high Fourier components of the pulse envelope. We can accommodate the objective and the cost by minimizing the modified functional

$$J_0[f(t),f^*(t)]=\overline{x^2}(T)-\bar{x}^2(T)+w\int_0^T dt|f(t)|^2. \tag{11}$$

The last term in Eq. (11) (the cost functional) subject to the normalization condition [Eq. (6)] limits the frequency spread of the pulse envelope, thereby limiting the high Fourier components of the pulse envelope. A positive parameter w which balances the degree of squeezing vs the bandwidth of the pulse envelope controls the importance we associate with this cost functional.

The objective functional of Eq. (11) is still too complicated because the $\bar{x}^2(T)$ term is quartic in the expansion coefficients $C_n(T)$. We therefore adopt a two-step optimization procedure.[6] In the first step, we solve the problem for a *fixed* $\bar{x}(T)$. In the second step, we repeat the optimization for different fixed values of $\bar{x}(T)$. The fixed-$\bar{x}(T)$ optimization problem is solved by adding to the $J_0[f(t),f^*(t)]$ functional two Lagrange multipliers λ and λ_1 which guarantee that the fixed-$\bar{x}(T)$ constraint and the normalization constraint of Eq. (6) are realized. We therefore seek stationary points of the modified functional

$$J[f(t),f^*(t)]=\overline{x^2}(T)-\lambda_1\bar{x}(T)-\lambda\sum_n |C_n(T)|^2 + w\int_0^T dt|f(t)|^2, \tag{12}$$

for which J_0 is minimal for a given λ_1 value.

The second stage of the optimization consists of repeating the fixed-$\bar{x}(T)$ optimizations for different $\bar{x}(T)$ values. By mapping $J_0[f(t),f^*(t)]$ as a function of $\bar{x}(T)$ (or λ_1), we can find the particular value of $\bar{x}(T)$ yielding the *global* minimum. The advantage of the two-step procedure is that we avoid working with the quartic J_0. Instead we work with $J[f(t),f^*(t)]$ which is *quadratic* in the $C_n(T)$ coefficients and hence can be minimized by linear algebraic methods.

It is easy to see that the optimal field for the fixed-$\bar{x}(T)$ problem, obtained by setting $\delta J/\delta f^*(t)$—the functional derivative of J with respect to $f^*(t)$—to zero, satisfies the equation

$$f(t)=-\frac{i\mu}{w}\sum_{n',n}\langle g|n'\rangle\exp(i\Delta_{n'}t)\tilde{M}_{n'n}C_n(T), \tag{13}$$

where

$$\tilde{M}_{n'n}=\exp(iE_{n'}T)M_{n'n}\exp(iE_nT) \tag{14}$$

with

$$M_{n'n}=(\hat{x}^2)_{n'n}-\lambda_1(\hat{x})_{n'n}-\lambda\delta_{n'n}. \tag{15}$$

Substituting Eq. (13) in Eq. (3), we obtain the following eigenvalue equations:

$$\sum_n Q_{kn}S_n(T)=\lambda S_k(T), \tag{16}$$

where the Q matrix is defined as

$$Q_{kn}=(\hat{x}^2)_{kn}-\lambda_1(\hat{x})_{kn}+w(\tilde{P}^{-1})_{kn} \tag{17}$$

and

$$\tilde{P}_{kn}=\exp(-iE_kT)P_{kn}\exp(iE_nT) \tag{18}$$

with

$$P_{kn}=\mu^2\langle k|g\rangle\frac{\exp[i(\Delta_n-\Delta_k)T]-1}{i(\Delta_n-\Delta_k)}\langle g|n\rangle. \tag{19}$$

The P_{kn} matrix is the one directly connected to the properties of the molecular absorption band.

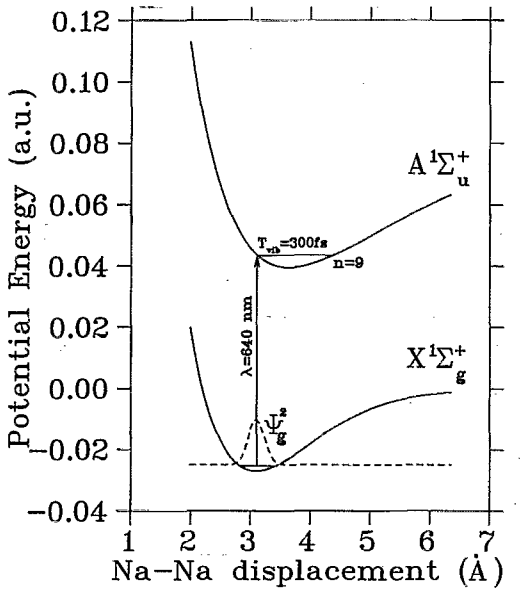

FIG. 1. The Na_2 potentials used in this work. Dashed line represents the ground state wave function.

Of all of the eigenvalues of Q, we choose the one for which J_0 is minimal. This λ value, and the S_n vector corresponding to it, are functions of λ_1 whose final value is determined in the second optimization stage.

III. OPTIMAL SQUEEZING IN Na_2

We illustrate the use of the above method by (computationally) demonstrating squeezing of vibrational wave packets in the Na_2 molecule. The computations are conducted on realistic potential curves, the lowest two shown in Fig. 1. Also shown in Fig. 1 is the square of the ground vibrational wave function in the ground ($X\ ^1\Sigma_g^+$) potential (whose equilibrium position is at $x=3.1$ Å). Ω the carrier frequency of the pump pulse is chosen to coincide with the "vertical" excitation frequency whose value ($\approx 15\,625\ cm^{-1}$) is essentially determined by the increase in the equilibrium distance of the $A\ ^1\Sigma_u^+$ state potential relative to the ground state potential.

The $n=9$ vibrational level of the $A\ ^1\Sigma_u^+$ state is closest in energy to the vertical excitation energy $E_g+\Omega$. The classical (anharmonic) period in the $n=9$ state is $T_{vib}=(2\pi)/(E_9-E_8)\simeq 300$ fs and the turning points of the motion are $x=2.9$ and 4.6 Å.

We obtain the vibrational eigenenergies and the corresponding eigenfunctions in the $A\ ^1\Sigma_u^+$ potential by the renormalized Numerov method[23] which we use to calculate the Franck–Condon integrals $\langle n|g\rangle$ by a Simpson-type quadrature. The expansion of Eq. (1) was truncated at $N_{max}\geqslant 50$ with the actual choice of N_{max} depending on the spectral width of the laser pulse under consideration.

Figure 2 displays the results of the optimized objective functional J_0 for two values of the weight factor w (measured in units of $w_0=(\mu^2 T_{vib}^2)/(2\pi\hbar m)$, where μ is the electronic dipole element and m is the reduced mass). The duration of the optimization interval is chosen equal to a full period ($T=T_{vib}$). Using the lower graphs of Fig. 2, it is possible to find the value of the Lagrange multiplier λ_1 corresponding to a given average coordinate position $\bar{x}$ of the packet. The upper graphs [Figs. 2(a) and 2(c)] allow one to

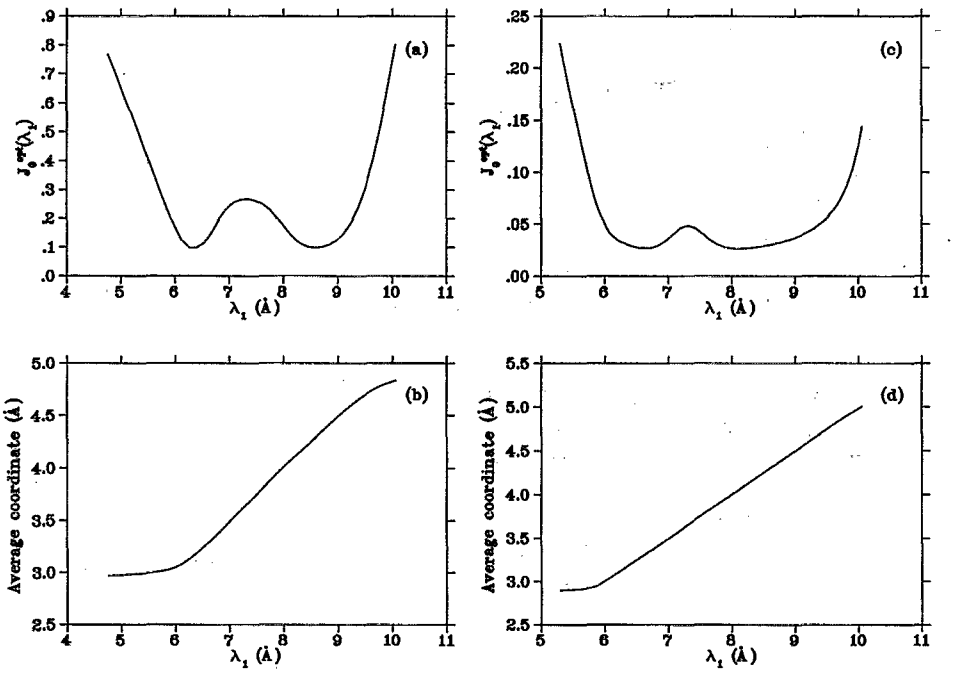

FIG. 2. The dependence of (a) and (c) $J[f(t),f^*(t)]$ of Eq. (12) and (b) and (d) $\bar{x}$ on λ_1 for (a) and (b) $w=10^{-2}$ and (c) and (d) 10^{-4}. The optimization time interval T equals the period of one vibration T_{vib}.

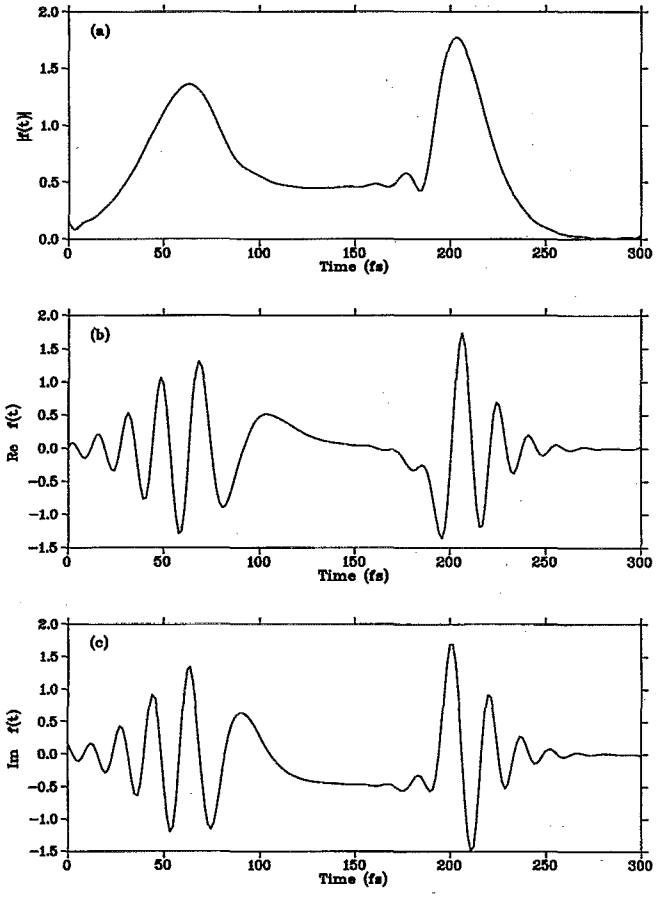

FIG. 3. Time dependence of the field (arbitrary units) which minimizes $J_0[f(t),f^*(t)]$ of Eq. (11) for $\bar{x}=4.5$ Å and $w=10^{-4}$. The optimization time is equal to the vibrational period $T_{\rm vib}$.

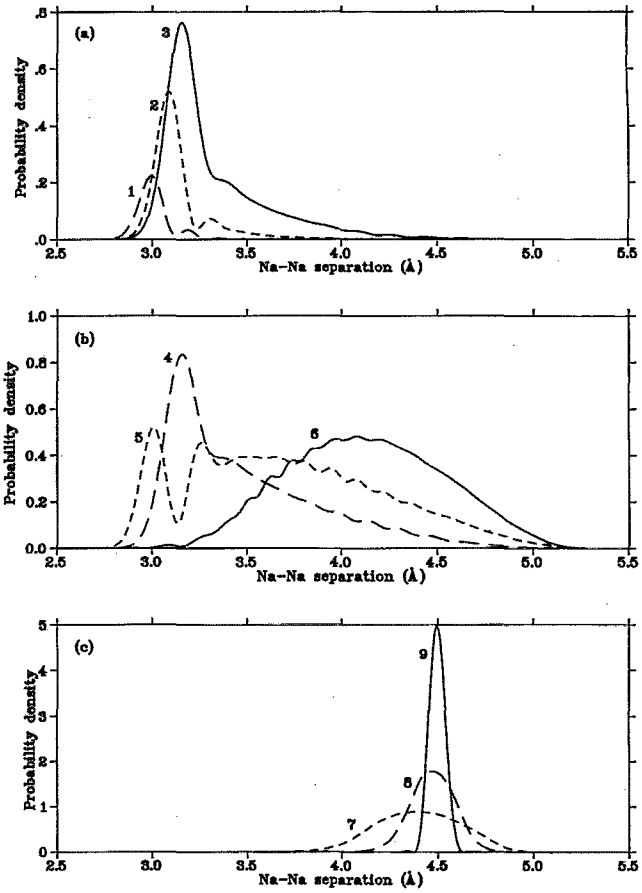

FIG. 4. Localization in space via generation of a momentum squeezed state. Shown is the time evolution of $|\Psi'(t)|^2$ for the field of Fig. 3. (a) $t/T=0.3$ (curve 1), 0.4 (curve 2), and 0.5 (curve 3); (b) $t/T=0.6$ (curve 4), 0.7 (curve 5), and 0.8 (curve 6); (c) $t/T=0.9$ (curve 7), 0.95 (curve 8), and 1.0 (curve 9).

find the value of $J_0^{\rm opt}$ as a function of λ_1 (and hence as a function of $\bar{x}$).

As shown in Fig. 2, for $w=10^{-2}$, the global minimum of $J_0^{\rm opt}$ is achieved at $\bar{x}=3.15$ Å and at $\bar{x}=4.4$ Å, i.e., near the classical turning points. The optimal field for a wave packet squeezed about $\bar{x}=4.5$ Å, i.e., near the right classical turning point is shown in Fig. 3. It consists of two distinct peaks and vanishes at the ends of the optimization interval.

The time evolution of the probability density $|\Psi'(t)|^2$ for the wave packet generated by this field is displayed in Fig. 4. The squeezing mechanism occurring here consists of alternations between squeezing in momentum space and coordinate space. As shown in Fig. 4, first a portion of the wave packet is created near the left turning point (at $x=2.9$ Å). This portion then spreads in coordinate space during its motion, until $t/T\simeq 0.8$, while at the same time localizing in momentum space. The trend is then reversed. After about one-quarter of the vibrational period, the wave packet localizes more and more in coordinate space, until, at $t/T=1$, maximal localization is achieved with $\sqrt{\mathscr{D}}=0.046$ Å.

That the localization thus achieved is in fact squeezing is shown in Fig. 5. There we compare the ground-state probability density (line 1) with a wave packet created from the ground state by a $\delta(t)$ pulse excitation at $t=T_{\rm vib}/2$ (line 2)

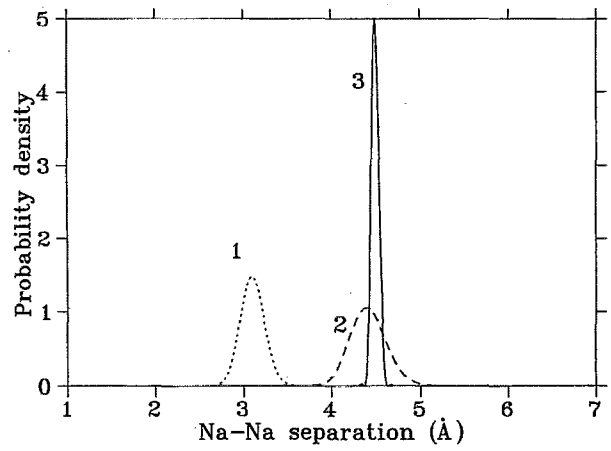

FIG. 5. The spatial distribution of $|\Psi_g|^2$ (curve 1), a wave packet created by $\delta(t)$ laser pulse at one-half of the vibrational period (curve 2) and the squeezed wave packet corresponding to the global minimum of $J_0[f(t),f^*(t)]$ of Eq. (11) at the end of the optimization interval $T=T_{\rm vib}$ (curve 3).

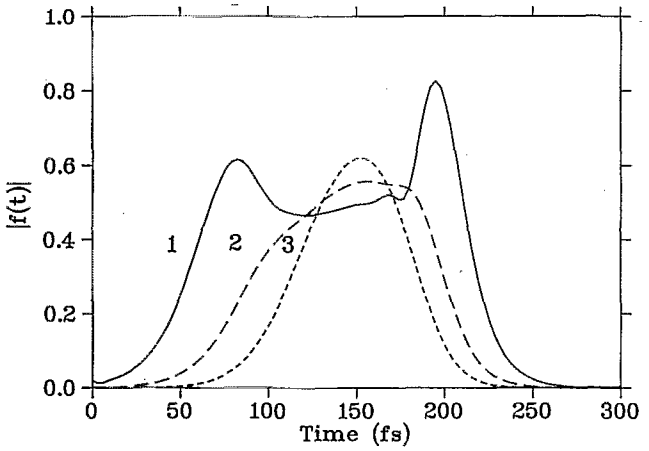

FIG. 6. The time dependence of the modulus of the optimal pulse envelope $|f(t)|$ for different values of the weight factor w. The optimization time is equal to the vibrational period T_{vib}.

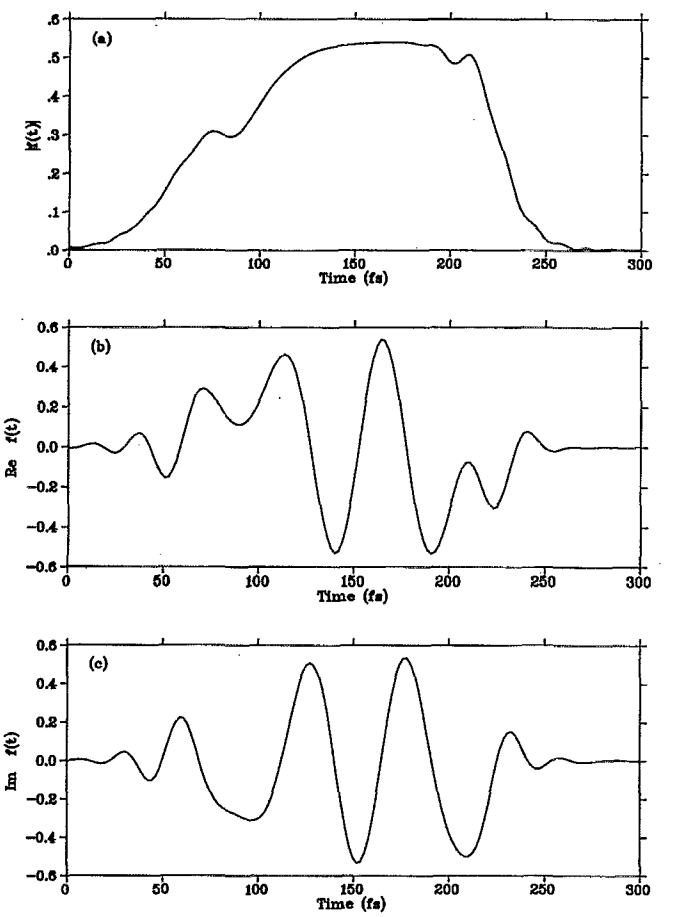

FIG. 7. The time dependence of (a) the modulus; (b) the real part; and (c) the imaginary part of the optimal pulse (arbitrary units) which minimizes $J_0[f(t),f^*(t)]$ of Eq. (11) ($w=10^{-2}$, $\bar{x}=4.1$ Å).

and our localized wave packet (line 3). The rms deviations in coordinate space for each wave function are $\sqrt{\mathscr{D}}=0.1$, 0.19, and 0.046 Å, respectively, i.e., squeezing by a factor of 2 has been achieved.

We next examine the role of the w parameter in the cost function of Eq. (11). As explained above, an increase in w biases against the excitation of vibrational states in the wings of the molecular absorption spectrum while smoothing the pulse envelope. In Fig. 6, we display three optimized fields which localize a wave packet about the same mean distance ($\bar{x}=4.5$ Å). Curves 1, 2 and 3, corresponding to w values of 10^{-3}, 10^{-2}, and 10^{-1}, yield wave packets whose rms deviations about $\bar{x}$ are 0.046, 0.055, and 0.069 Å, respectively. Obviously, smoothness is achieved at the expense of localization. Note, however, that even the smoothest pulse of curve 3 manages to squeeze the wave packet, i.e., localize it beyond the ground state.

The squeezing mechanism operating in the case shown in Fig. 4, in which momentum space squeezing alternates with coordinate space squeezing, is by no means the only way squeezing can be achieved. We find that different squeezing mechanisms are operative with different choices of $\bar{x}$. One of the most effective mechanisms is the *interference between two colliding wave packets.*

In Fig. 7, we show an optimized laser field which creates a wave packet centered away from the right turning point (at $\bar{x}=4.1$ Å). The time evolution of $|\Psi'(t)|^2$ is shown in Figs. 8(a)–8(c). As before, the probability density is first generated near the left turning point (at $x=2.9$ Å). However, in this case, the optimized wave packet does not spread out to the same extent as the wave packet of Fig. 4. Rather, it moves to the right as a whole. After some time ($t\approx 0.6T$), the field generates an additional distinct wave packet on the left which also starts moving to the right while the front wave packet reaches the right turning point and begins moving to the left [Fig. 8(b)]. Finally [Fig. 8(c)], the two wave packets collide near $x=3.7$ Å and interfere to form a highly localized wave packet whose rms deviation of 0.06 Å indicates that squeezing has been attained. A similar mechanism was observed for harmonic oscillators.[6]

In the above two scenarios, squeezing is attained largely as a result of the presence of two turning points. It is interesting to examine the possibility of squeezing in the absence of a right turning point, a case of particular importance for excitation to dissociative states. We can do so by shortening the optimization period and optimize the wave packet about an $\bar{x}$ value near the left turning point. In this way, the effect of the right turning point is minimal.

The results of such an optimization for $T=0.5T_{\text{vib}}\approx 150$ fs, $\bar{x}=3.4$ Å, and $w=10^{-2}$) are presented in Figs. 9–11. In Fig. 9(a), we show the optimal field and in Fig. 10 the ensuing time evolution of $|\Psi'(t)|^2$. We see that after an initial pump stage, in which a broadened Gaussian looking wave packet is formed on the upper potential [Fig. 10(a)], the wave packet is seen to gradually narrow down as it moves away from the Franck–Condon region [Figs. 10(b) and 10(c)]. At the end of the optimization time, a localized wave packet is formed near $\bar{x}=3.4$ Å. Although the degree of localization is roughly that of the ground state ($\sqrt{\mathscr{D}}=0.1$ Å), the optimized wave packet avoids (and even overcomes) the usual dispersive broadening of freely evolving wave packets.

The case studied here falls under the category of wave

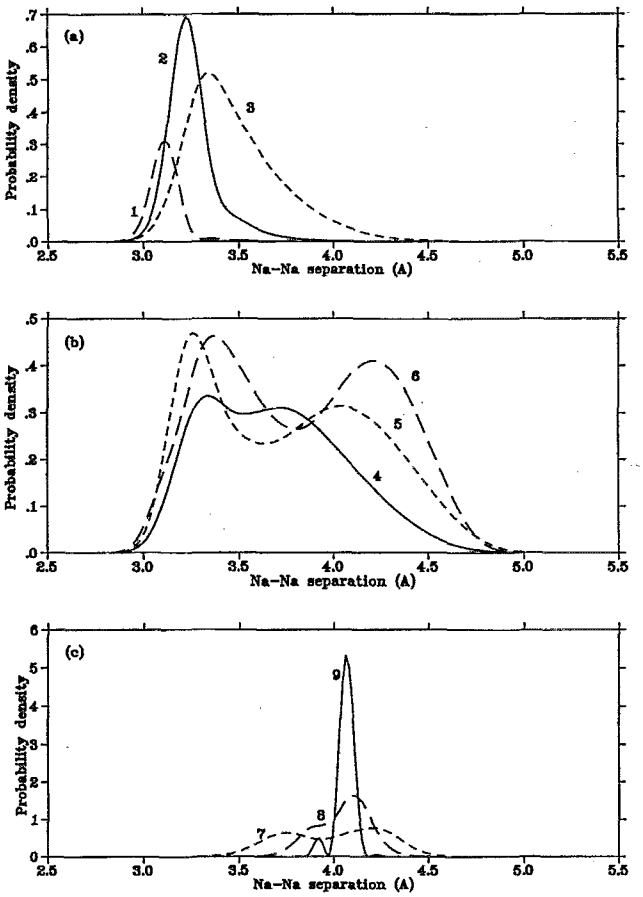

FIG. 8. Squeezing via interference of two colliding wave packets. Shown is the time evolution of $|\Psi'(t)|^2$ for the field of Fig. 7. (a) $t/T=0.3$ (curve 1), 0.4 (curve 2), and 0.5 (curve 3); (b) $t/T=0.6$ (curve 4), 0.7 (curve 5), and 0.8 (curve 6); (c) $t/T=0.9$ (curve 7), 0.95 (curve 8), and 1.0 (curve 9).

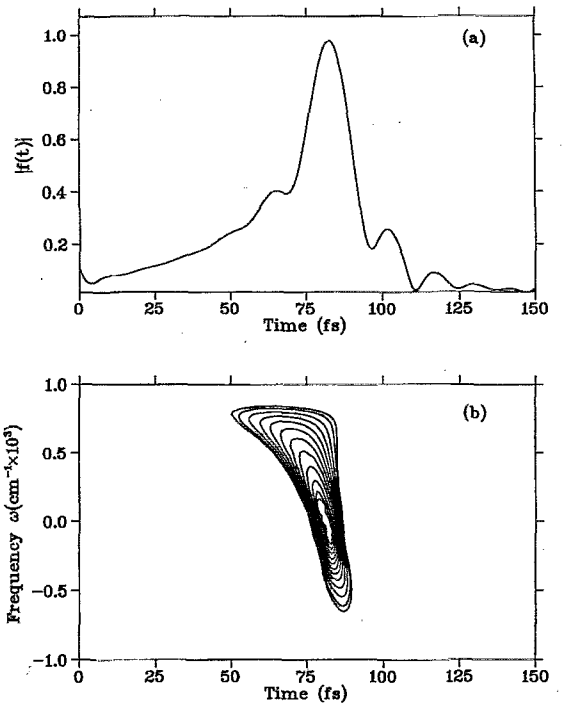

FIG. 9. The optimal field which minimizes $J_0[f(t),f^*(t)]$ of Eq. (11) for $T=0.5T_{\rm vib}$, $\bar{x}=3.4$ Å, and $w=10^{-2}$. (a) The time dependence of the modulus of the optimal pulse (arbitrary units). (b) The Wigner representation of the optimal field as calculated with Eq. (23).

packets known as "contractive states." Such states were studied before for the case of a free evolution.[24,25] The underlying reasons for the contraction are best explained by looking at the excited state probability current in a frame moving with the average velocity of the wave packet given as

$$\bar{v}=\frac{\bar{p}}{m}=\frac{-i}{m}\int dx\ \Psi'^*(x,t)\frac{\partial\Psi'(x,t)}{\partial x}. \tag{20}$$

The probability flux in this frame is given as

$$j(x,t)_{\rm mov}=j(x,t)-|\Psi'|^2\bar{v}, \tag{21}$$

where

$$j(x,t)\equiv\frac{-i}{2m}\left(\Psi'^*\frac{\partial\Psi'}{\partial x}-\Psi'\frac{\partial\Psi'^*}{\partial x}\right). \tag{22}$$

When reflection from the right turning point occurs (as in the previous cases), the space-fixed $j(x,t)$ changes sign. In the present case, however, no reflection occurs, and $j(x,t)$ is always positive. In contrast, $j(x,t)_{\rm mov}$, shown in Fig. 11 for $t=0.7T$ (at the peak of the pulse) is both positive and negative. This indicates that the wave packet is composed of two parts—one moving to the right and one moving to the left in the moving frame. These two motions, which have the effect of narrowing down the wave packet, correspond in the space-fixed frame to the overtaking of the front of the wave packet by its tail. At the end of the optimization interval $t=T$, the wave packet spreads again because the tail (which is now in the front) continues to move faster than the front (which is now in the rear).

An additional insight into the physics of the squeezing mechanism is provided by the time-frequency Wigner distribution function for the field amplitude, which is defined as[26,27]

$$W(t,\omega)=\frac{1}{\pi}\int_{-\infty}^{\infty}d\tau\ e^{i2\omega\tau}f^*(t+\tau)f(t-\tau). \tag{23}$$

A contour plot of the time-frequency Wigner function of the optimal laser field obtained for $w=0.01$ and $\bar{x}=3.4$ Å is shown in Fig. 9(b). Here, the frequency ω is measured relative to the laser center frequency Ω.

As seen in Fig. 9(b), the optimal pulse has a rather broad spectral bandwidth due to the considerable frequency chirp. High frequency components of the field come earlier than the low frequency components, i.e., the pulse is red chirped. The reason for the negative chirp is rather clear. When a molecule is excited from the ground state E_g by one of the laser modes ω, it appears on the upper potential with energy E, $E=E_g+\hbar\omega$, as a wave function peaking near the classical turning point $x_{\rm cl}(E)$. The higher the frequency, the larger the time of the classical motion from $x_{\rm cl}$ to $\bar{x}$ (for $\bar{x}$ on the left side of the equilibrium position). The red chirp of the laser

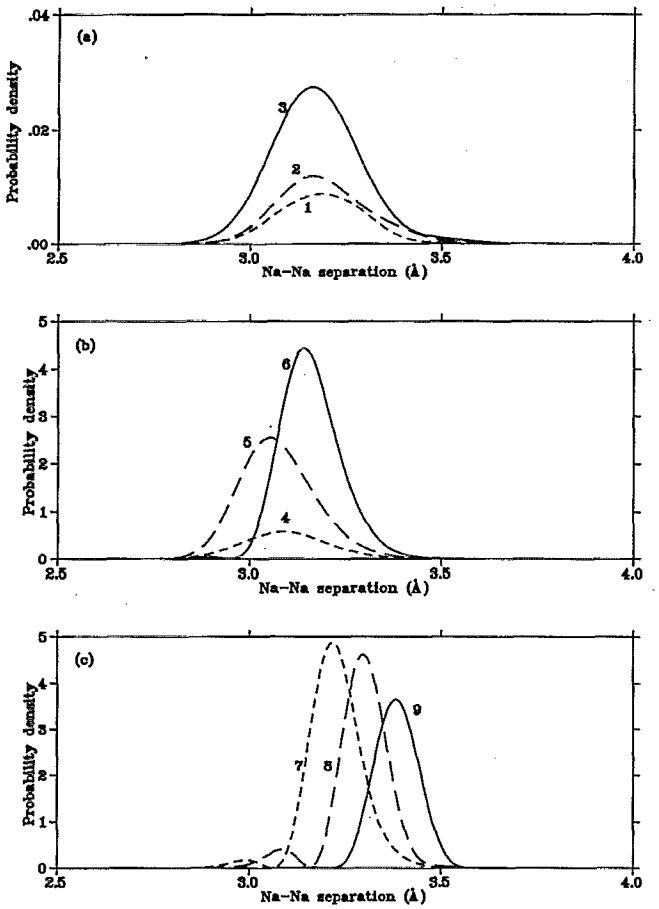

FIG. 10. Squeezing by the overtaking of a slow front. Shown is the time evolution of $|\Psi'(t)|^2$ for the field of Fig. 9. (a) $t/T=0.3$ (curve 1), 0.4 (curve 2), and 0.5 (curve 3); (b) $t/T=0.7$ (curve 4), 0.8 (curve 5), and 0.85 (curve 6); (c) $t/T=0.9$ (curve 7), 0.95 (curve 8), and 1.0 (curve 9).

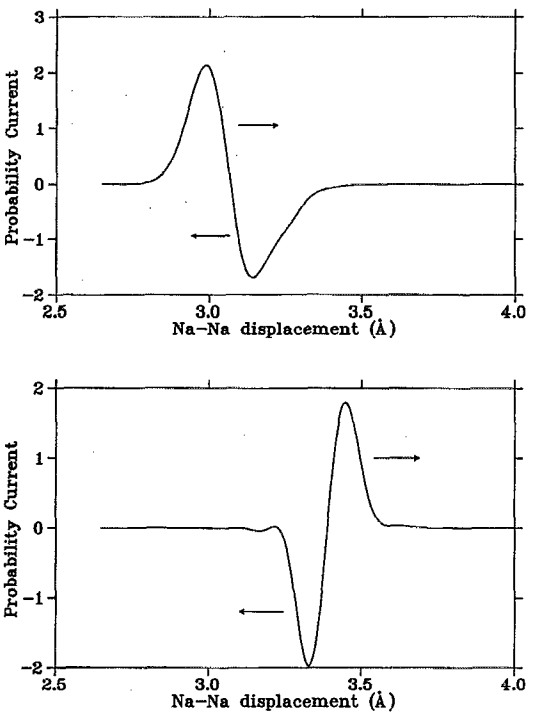

FIG. 11. Dependence of the probability current in the moving frame as calculated from Eq. (21) on the Na–Na displacement at the different moments of time (a) $t/T=0.7$; (b) $t/T=1$.

pulse compensates for this difference in transit time and leads to the focusing of the wave function at $x=\bar{x}$.

The idea to use chirped pulses for shortening of wave packets was previously suggested in Refs. 14 and 28. In contrast to the present work, in Ref. 14 focusing of outgoing wave packets in I_2 was obtained by *blue chirping*. In that case, squeezing was achieved at a large interatomic distance, where the classical motion is almost free.

IV. CONCLUSIONS

In this paper, we have applied the optimal squeezing method to the study of squeezing in a realistic system—the Na_2 molecule. Our study has revealed three main squeezing scenarios: alternations between momentum space and configuration space localizations, interference between colliding wave packets, and a slow front being overtaken by a fast tail. Each squeezing scenario has been shown to be relevant to different target average displacements or to different target times.

From the "engineering" point of view, we have demonstrated by optimal squeezing that it is possible to generate vibrational wave packets squeezed about any desired accessible displacement on the upper potential curve, while at the same time using smooth-looking, easy-to-fabricate pulses.

Future applications will deal with squeezing in *time* and the use of molecular emission as a means of attaining pulse compression.

ACKNOWLEDGMENTS

This research was supported by grants from the Israel Ministry of Science and the Arts and the Israel Ministry of Absorption, and by the U.S.–Israel Binational Science Foundation Grant No. 92-335.

[1] See, e.g., special issues on squeezing and nonclassical light, J. Opt. Soc. Am. B **4** (1987); J. Mod. Opt. **34** (1987).
[2] J. Janszky and Y. Y. Yushin, Opt. Commun. **59**, 151 (1986).
[3] J. Janszky and An. V. Vinogradov, Phys. Rev. Lett. **64**, 2771 (1990).
[4] J. Janszky, T. Kobayashi, and An. V. Vinogradov, Opt. Commun. **76**, 30 (1990).
[5] W. Schleich, M. Pernigo, and Fam Le Kien, Phys. Rev. A **44**, 2172 (1991).
[6] I. Averbukh and M. Shapiro, Phys. Rev. A **47**, 5086 (1993).
[7] D. J. Tannor and S. A. Rice, J. Chem. Phys. **83**, 5013 (1985); Adv. Chem. Phys. **70**, 441 (1988).
[8] D. J. Tannor, R. Kosloff, and S. A. Rice, J. Chem. Phys. **85**, 5805 (1986).
[9] S. Shi, A. Woody, and H. Rabitz, J. Chem. Phys. **88**, 6870 (1988).
[10] A. Pierce, M. Dahleh, and H. Rabitz, Phys. Rev. A **37**, 4950 (1988).
[11] R. Kosloff, S. A. Rice, P. Gaspard, S. Tersigni, and D. J. Tannor, Chem. Phys. **139**, 201 (1989).
[12] C. D. Schweiters and H. Rabitz, Phys. Rev. A **44**, 5224 (1991).
[13] R. S. Judson and H. Rabitz, Phys. Rev. Lett. **68**, 1500 (1992).
[14] J. L. Krause, R. M. Whitnell, K. R. Wilson, Y. Yan, and S. Mukamel, J. Chem. Phys. **99**, 6562 (1993); J. L. Krause, R. M. Whitnell, K. R. Wilson, and Y. Yan, in *Femtosecond Chemistry*, edited by J. Manz and L. Wöste (Chemie, Berlin, 1994).

[15] A. H. Zewail, Science **242**, 1645 (1988); A. H. Zewail and R. B. Bernstein, Chem. Eng. News **66**, 24 (1988).
[16] T. J. Dunn, J. N. Sweetser, I. A. Walmsley, and C. Radziewicz, Phys. Rev. Lett. **70**, 3388 (1993).
[17] A. H. Zewail, Faraday Discuss. Chem. Soc. **91**, 207 (1991).
[18] J. L. Krause, M. Shapiro, and R. Bersohn, J. Chem. Phys. **94**, 5499 (1991).
[19] M. Shapiro, J. Phys. Chem. **97**, 7396 (1993).
[20] H. Okabe, *Photochemistry of Small Molecules* (Wiley, New York, 1978).
[21] C. V. Shank, in *Ultrashort Laser Pulses; Applications*, edited by W. Kaiser (Springer, Berlin, 1988).
[22] A. M. Weiner, J. P. Heritage, and R. N. Thurston, Opt. Lett. **11**, 153 (1986); A. M. Weiner and J. P. Heritage, Rev. Phys. Appl. **22**, 1619 (1987).
[23] B. R. Johnson, J. Chem. Phys. **67**, 4086 (1977)
[24] H. P. Yuen, Phys. Rev. Lett. **51**, 719 (1983).
[25] H. Higurashi, Prog. Theor. Phys. **84**, 28 (1990).
[26] E. P. Wigner, Phys. Rev. **40**, 749 (1932).
[27] M. Hillery, R. F. O'Connell, M. O. Scully, and E. P. Wigner, Phys. Rep. **106**, 193 (1984).
[28] L. D. Noordam, H. G. Muller, A. ten Wolde, and H. B. van Linden van den Heuvell, J. Phys. B **23**, L115 (1990).